Transfer function models and sensitivity analysis

Ajay M. Koshti
NASA Johnson Space Center, Houston, U. S. A.

ABSTRACT

In many situations, real or induced flaws such as tight cracks with known morphology cannot be manufactured in part configuration specimens or in real parts. Typically, fatigue cracks are manufactured in simple geometry specimens such as flat plates, dog-bone shaped flat or round specimens. If a nondestructive evaluation (NDE) technique is required to provide a reliably detectable target flaw size denoted as $a_{90/95}$ for induced flaws in real part, then the direct method for qualifying the NDE procedure is to use the appropriate induced flaw specimens and perform probability of detection analysis using these flaws. This can be described as direct POD demonstration testing, which may follow guidelines of MIL-HDBK-1823. This paper considers a case, where induced flaws are not available in part configuration specimens. Therefore, a direct POD demonstration study cannot be undertaken. In such situation, general practice for NDE procedure qualification is to use artificial flaws in simple geometry and part configuration specimens, and induced flaws in the chosen simple geometry specimens. Signal response data is taken on all sets of artificial and induced flaws. NDE procedure testing on induced flaw in simple geometry specimen is called NDE demonstration testing here. A transfer function NDE procedure qualification method for forward case calculates predicted induced flaw size for demonstration using a chosen target flaw size. Another transfer function method for inverse case, calculates the target flaw size using a given demonstration flaw size. The transfer function analysis assumes relationship of artificial flaw signal responses in real parts and simple geometry specimens; and induced flaw responses in simple geometry specimens to induced flaws in real parts. The signal response transfer relationships model should be defined before transfer function models can be devised. Assuming that the signal response transfer relationships model is valid, forward and inverse case transfer function methods have been devised. Because of lack of signal response data from induced flaws in real part, 90/95% POD/confidence (P/C) cannot be demonstrated directly. However, the transfer function method may be assessed using simulation to evaluate whether the resulting target flaw size or demonstration flaw size provides adequate confidence to the assumed signal response transfer relationships model. Therefore, the transfer function approach is a risk assessment approach. Both the signal response transfer relationships model and the transfer function model are important in managing risk in results provided by the transfer function NDE technique qualification or assessment. The signal response transfer relationships model needs to be validated with empirical data and then transfer function model needs to be validated for desired P/C on case-by-case basis.

Keywords: Nondestructive evaluation, probability of detection, transfer function

1. INTRODUCTION

MIL-HDBK-1823A[1] and associated mh1823[2] software address NDE POD testing for two types of datasets. The first type of dataset is that of the signal response "$\hat{a}$" (read as a-hat) versus known flaw size "a". In analyzing such data, the $\hat{a}$ data is represented on the y-axis and the "a" data on the x-axis and the data may be transformed using a logarithmic function, if needed, to provide a linear relationship around the signal response decision threshold level. A generalized linear model (GLM) is fitted to the data using maximum likelihood estimate (MLE) for analysis. In this analysis, noise data, defined as the signal response in a region where there is no flaw, is also obtained. The noise data is used to estimate false call rate or probability of false positive calls (POF).

The second type of dataset considered is that of hit-miss data, which contains the known flaw size and the corresponding detection result i.e., hit or miss. For numerical analysis, a hit is assigned a numerical value of 1 while a miss has numerical value of 0. False call data (i.e., a hit is recorded where no flaw exists) is also recorded and used to determine the POF using the Clopper-Pearson binomial distribution function. Typically, POD increases with increasing flaw size and POF decreases with increasing flaw size. POF shall be required to be less than a certain limit to prevent adverse impacts on cost and schedule necessary to take corrective actions to address the false positive calls. ASTM E2862[3] also provides a hit-miss

POD data analysis method that is consistent with MIL-HDBK-1823A. There are other POD analysis approaches that are not covered by MIL-HDBK-1823A. The Binomial point estimate method of verifying reliably detectable flaw size is given by Rummel[4].

Current work is in probability of detection (POD) analysis using tolerance intervals[5,6]. This work is limited to POD analysis and simulation approach for single-hit limited sample POD[7] or LS POD. Broadly, LS POD covers signal response-based data for both single-hit and multi-hit POD applications including modeling of transfer functions[7-15]. Smaller sample size is usable in LS POD analysis. In practice, signal responses from smaller sample size of flaws may not be random to the population. LS POD assumes that the sample is randomly drawn from the population. Generally, a sample is drawn from one end of the signal response population where average and standard deviation of signal responses are assumed to be lower than that of the population. These samples are called worst case signal responses[9]. Koshti[10,16] provides model for transfer function method using linear fit to data. Transfer function model is used to qualify or validate NDE procedure in detecting flaws reliably. This paper advances the work by considering an exponentially saturating signal response as simulated data for assessing effectiveness of the transfer function method and performing a parametric assessment. The transfer function method can use a linear or second order polynomial fit to signal response data in this work. The transfer function method can use data that has high correlation coefficient to a linear or second order fit. In the simulation, parameters for sample data can be changed to assess effectiveness of transfer function results. A method of transfer function sensitivity analysis using simulated data is provided here. NESC Guidebook[16] provides guidelines for implementation of the transfer function method for both forward and inverse cases and provides extensive list of relevant references. Transfer function analysis method using user provided data is also provided here.

2. SIGNAL RESPONSE TRANSFER RELATIONSHIPS

Signal response transfer relationships model will be defined before explaining transfer function models. There are four signal response data types denoted as Data (type) 1, Data (type) 2, Data (type) 3 and Data (type) 4 respectively. “x” is used to denote flaw size. Nomenclature for signal responses is provided below.

Table 1: Nomenclature for signal response data sets.

		Flaw Type	
		Artificial or Machined Flaw (e.g., EDM, subscript e)	Induced Flaw (e.g., crack, subscript c)
Specimen Geometry	Simple Geometry (subscript 1)	Data 1: y_{e1}	Data 3: $y_{c,1}$
	Part Configuration or real part (subscript 2)	Data 2: $y_{e,2}$	Data 4: $y_{c,2}$

Note that subscript “1” is used for simple geometry specimens and subscript “2” is used for part or part configuration specimens. An example of simulated data for signal response transfer relationships model is provided below.

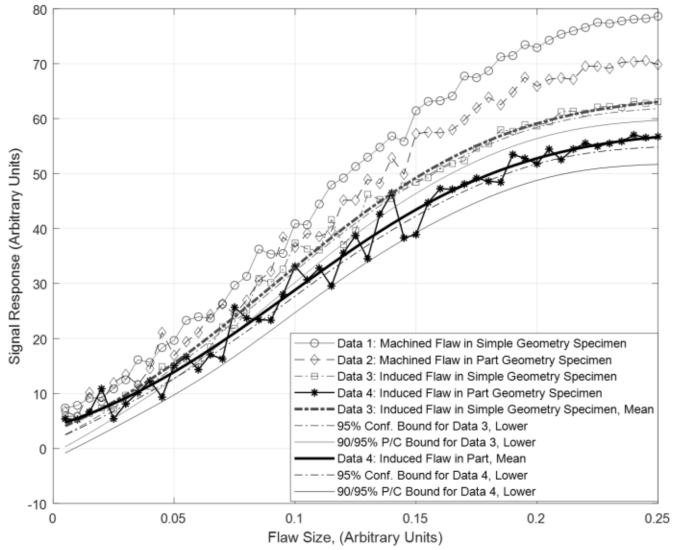

Fig. 1: An example of simulated data for signal response transfer relationships model

In above example, all data sets have upper saturation limits. The data functions are modeled using a saturating exponential function i.e., error function. However, parameters of this function can be chosen such that signal response will be approximately linear in the flaw range of interest. Signal saturation is quite common in NDE procedures. The transfer model is developed for linear signal responses, therefore non-linearity in signal responses will impose limits on applicability of the transfer function model presented here. Simulation method provided here can explore the limits of applicability of transfer function models for a given application. Signal response variation increases with flaw size but reduces as signal value approaches the saturation limit. This feature is modeled in this simulation as it may be observed in practice. Although, if desired, this feature may be suppressed in the model. The signal response transfer relationships model can be devised using following inputs and relationships.

Table 2: Signal response transfer relationships model inputs and their relationships

Input Parameter No.	Description of Input	Notation	Example Values	Comments
1	Amplitude (% full screen height or % FSH)	$\overline{y}_{e1,max}$	80	Sets saturation limit for Data 1.
2	Noise, standard deviation (% FSH)	σ_1	0.2	For simple geometry, subscript 1 is used and for part, subscript 2 is used.
3	Noise ratio, part-to-simple geometry (% FSH)	$R = \frac{\sigma_2}{\sigma_1}$ (1A)	1.5	$\sigma_2 = R\sigma_1$ (1B)
4	EDM size variation equivalent to signal response standard deviation (% FSH)	σ_{e1}^{x}	0.03	
5	EDM flaw size standard deviation ratio, part-to-simple geometry (% FSH)	$f_A = \frac{\sigma_{e2}^{x}}{\sigma_{e1}^{\Delta x}}$ (2A)	1.5	$\sigma_{e2}^{x} = f_A\sigma_{e1}^{x}$ (2B)
6	Induced flaw signal standard deviation ratio, part-to-simple geometry (% FSH)	$f_B = \frac{\sigma_{c1}^{x}}{\sigma_{e1}^{x}}$ (3A)	2.0	$\sigma_{c1}^{x} = f_B\sigma_{e1}^{x}$ (3B) $\sigma_{c2}^{x} = f_A f_B\sigma_{e1}^{x}$ (4)
7	Mean signal response ratio, part-to-simple geometry (% FSH)	$R_A = \frac{\overline{y}_{e2,max}}{\overline{y}_{e1,max}}$ (5)	0.9	
8	Mean signal response ratio, Crack-to-EDM (% FSH)	$R_B = \frac{\overline{y}_{c1,max}}{\overline{y}_{e1,max}}$ (6)	0.8	$\overline{y}_{c2,max} = R_A R_B \overline{y}_{e1,max}$ (7)

9	Minimum flaw size (arbitrary units)	$x_{c2,min}$	0.005	Also applicable for Data 1, Data 2, Data 3, and Data 4.
10	Maximum flaw size (arbitrary units)	$x_{c2,max}$	0.4	Also applicable for Data 1, Data 2, Data 3, and Data 4.
11	Flaw size spacing (arbitrary units)	$\Delta_{e1}^{x} = \Delta_{e2}^{x} = \Delta_{c1}^{x} = \Delta_{c2}^{x}$ (8)	0.005	
12	Flaw size for 50% of saturated signal response function (arbitrary units)	$x_{e1}^{50} = x_{e2}^{50} = x_{c1}^{50} = x_{c2}^{50}$ (9)	0.1	$x_{norm} = \frac{(x - x_{e1}^{50})}{\sigma_{e1}^{x}}$ (10)
13	Standard deviation of saturated signal response function (% FSH)	$\sigma_{e1}^{x} = \sigma_{e2}^{x} = \sigma_{c1}^{x} = \sigma_{c2}^{x}$ (11)	0.1	

Signal response models are given by Eq. (12) through Eq. (15).

$$y_{e1} = \frac{\overline{y}_{e1,max}}{2}(1 + erf\ (x_{norm} + randn(\sigma_{e1}^{x}))) + randn(\sigma_1), \tag{12}$$

$$y_{e2} = \frac{\overline{y}_{e2,max}}{2}(1 + erf\ (x_{norm} + randn(\sigma_{e2}^{x}))) + randn(\sigma_2), \tag{13}$$

$$y_{c1} = \frac{\overline{y}_{c1,max}}{2}(1 + erf\ (x_{norm} + randn(\sigma_{c1}^{x}))) + randn(\sigma_1), \text{ and} \tag{14}$$

$$y_{c2} = \frac{\overline{y}_{c2,max}}{2}(1 + erf\ (x_{norm} + randn(\sigma_{c2}^{x}))) + randn(\sigma_2), \tag{15}$$

where,

erf = error function, and

randn = random number generator function with Gaussian distribution.

Note that for mean value of signal responses, Eq. (12) through Eq. (15) are simplified as Eq. (16) through Eq. (19).

$$\overline{y}_{e1} = \frac{\overline{y}_{e1,max}}{2}(1 + erf\ (x_{norm})). \tag{16}$$

$$\overline{y}_{e2} = \frac{\overline{y}_{e2,max}}{2}(1 + erf\ (x_{norm})). \tag{17}$$

$$\overline{y}_{c1} = \frac{\overline{y}_{c1,max}}{2}(1 + erf\ (x_{norm})). \tag{18}$$

$$\overline{y}_{c2} = \frac{\overline{y}_{c2,max}}{2}(1 + erf\ (x_{norm})). \tag{19}$$

Using Eq. (7) and Eq. (16) through Eq. (19), it can be shown that,

$$\overline{y}_{c2} = \frac{\overline{y}_{c1}\overline{y}_{e2}}{\overline{y}_{e1}}. \tag{20}$$

Eq. (4) can be rewritten as,

$$\sigma_{c2}^{x} = \frac{\sigma_{c1}^{x}\sigma_{e2}^{x}}{\sigma_{e1}^{x}}. \tag{21}$$

Eq. (20) and Eq. (21) are the basic assumptions of the signal response transfer relationships model. Taking derivatives of Eq. (20), following expression is obtained.

$$\frac{\partial\overline{y}_{c2}}{\overline{y}_{c2}} = \frac{\partial\overline{y}_{c1}}{\overline{y}_{c1}} + \frac{\partial\overline{y}_{e2}}{\overline{y}_{e2}} - \frac{\partial\overline{y}_{e1}}{\overline{y}_{e1}}. \tag{22}$$

The three signal response quantities are independent, and they are assumed to have Gaussian distributions. Therefore, combined fractional error can be given by summation of quadrature formula instead of Eq. (22).

$$\frac{\Delta\overline{y}_{c2}}{\overline{y}_{c2}} = \sqrt{\left(\frac{\Delta\overline{y}_{c1}}{\overline{y}_{c1}}\right)^2 + \left(\frac{\Delta\overline{y}_{e2}}{\overline{y}_{e2}}\right)^2 + \left(\frac{\Delta\overline{y}_{e1}}{\overline{y}_{e1}}\right)^2} \tag{23}$$

Eq. (23) simplifies as,

$$\Delta\overline{y}_{c2} = \sqrt{\left(\Delta\overline{y}_{c1}\right)^2 + \left(\Delta\overline{y}_{e2}\right)^2 + \left(\Delta\overline{y}_{e1}\right)^2} \text{ for } \overline{y}_{c2} = \overline{y}_{c1} = \overline{y}_{e2} = \overline{y}_{e1}. \tag{24}$$

Eq. (23) simplifies as,

$$\Delta\overline{x}_{c2} = \sqrt{\left(\Delta\overline{x}_{c1}\right)^2 + \left(\Delta\overline{x}_{e2}\right)^2 + \left(\Delta\overline{x}_{e1}\right)^2} \text{ for } \overline{x}_{c2} = \overline{x}_{c1} = \overline{x}_{e2} = \overline{x}_{e1}. \tag{25}$$

These are basic assumptions of the transfer response relationships. In Fig. 1, error function fits are shown for Data 3 and Data 4 with 95% confidence on fit; and 90% lower data bound (or probability) with 95% confidence i.e., lower 90/95% P/C. It should be remembered that the fit and bounds are influenced by the selected data range. The saturating portion of the data may bring the data bounds closer, indicating that more datapoints are outside in the middle portion of the curve. Thus, statistical curve fitting to assess confidence bounds may have limitations if signal response variance is also a function of the flaw size. Input parameters 1 through 13 with their chosen values and Eq. (1) through (25) describe a chosen signal response transfer model completely.

3. DESCRIPTION OF FORWARD AND INVERSE CASES FOR TANSFER FUNCTION

For forward case of transfer function, a target flaw size to be detected reliably in the part $x_{c2,90/95}^{target}$ is provided. Here, objective is to determine demonstration flaw size for simple geometry specimens. Once the demonstration flaw size is known, a demonstration test can be set-up to test operators using Binomial point estimate method or LS POD method. Alternately, a range of flaws containing the demonstration flaw size can be manufactured and used in the operator demonstration test using MIL-HDBK-1823 POD analysis methods. If the operator demonstrates minimum 90/95% P/C to detect the demonstration size flaw, then the operator is assumed have demonstrated high reliability in detecting the target size flaw in the part. The operator also needs to supplement the demonstration by detecting relevant same size flaws belonging to Data 2 type. This will verify that the NDE procedure provides acceptable flaw detectability in part configuration specimens. Thus, the forward transfer method is used to qualify a flaw size for NDE procedure demonstration using induced flaws in simple geometry specimens.

For inverse case, induced flaw size with 90/95% P/C for demonstration in simple geometry specimens is known. Here, objective is to determine smallest reliably detectable flaw size in part i.e. $x_{c2,90/95}^{est}$ using the NDE procedure at hand. Here, the exact procedure that was used in the demonstration may not be known, but it is assumed that the NDE procedure used in demonstration is similar to the procedure under evaluation. The procedure under evaluation is assumed to be equivalent or better in terms of flaw detectability compared to the one used in the demonstration.

Generally, there is a fracture control requirement to detect a flaw size with minimum 90/95% P/C. Here, this flaw size is denoted by $a_{c2,90/95}^{req}$. Both forward and inverse transfer functions are used in relation to this flaw size such that the NDE procedure qualified flaw size should be smaller than the requirement flaw size. It should be remembered that determining smallest reliably detectable flaw size (inverse case) or 90/95% P/C demonstration flaw size for a given target flaw size (forward case) do not provide P/C of 90/95% directly for the qualified flaw size. The transfer function method can provide estimates based on acceptance of risk in using the signal response transfer relationships model and transfer function models.

4. METHOD FOR ASSESSING EFFECTIVITY OF FORWARD TRANSFER FUNCTION MODEL

Having accepted the signal response transfer relationships model, simulated data will be used to assess effectivity of the forward transfer function model as an example.

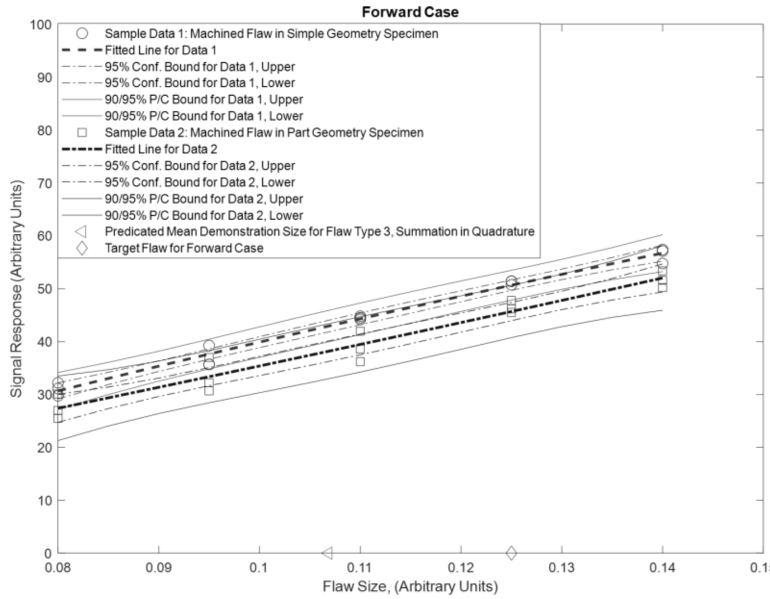

Fig. 2: Fitted second order polynomials through sample Data 1 and Data 2

Here, sampling protocol for Data 1 and Data 2 needs to be selected. The flaw sizes in the sample will be equally spaced. As an example, 5 flaw sizes are chosen and 3 replicates at each flaw size (i.e., 5 sizes x 3 replicates) are chosen. One may choose other sampling schemes such as 3 x 3 or 4 x 4. For curve fitting through these data points, either a straight line or a second order polynomial is available for this exercise. Second order polynomial is chosen in this example. Fig. 2 and 3 illustrate an example of the forward case.

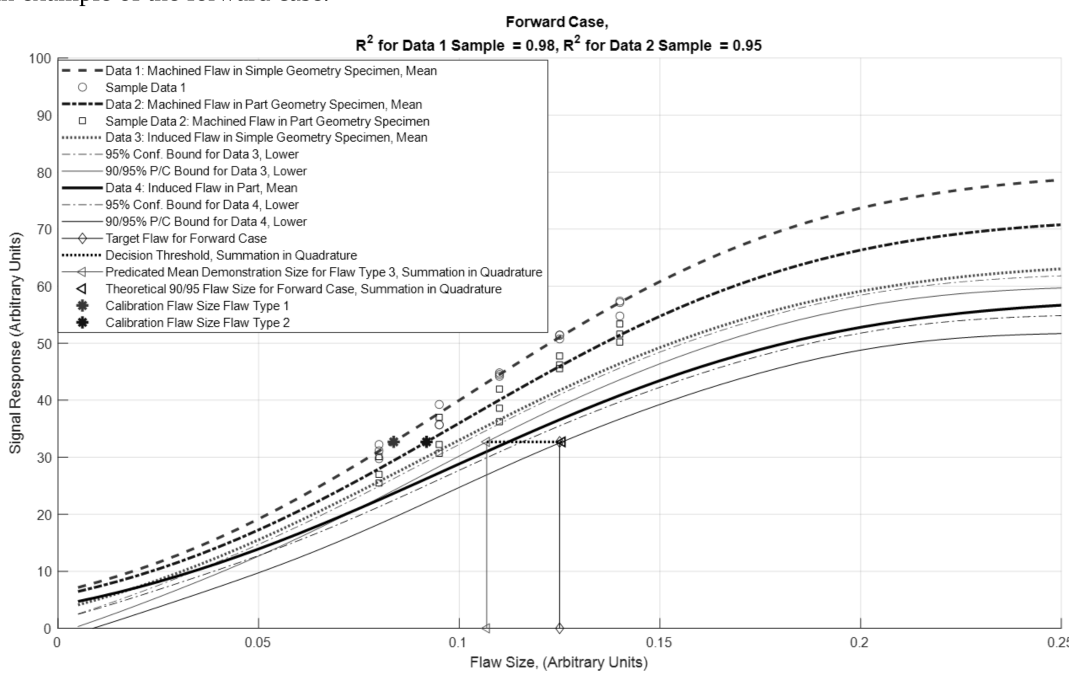

Fig. 3: Sample Data 1 and Data 2 overlaid on the respective mean curves and analysis for forward case

Regression coefficient R^2 values for Data 1 sample and Data 2 sample are provided in Fig 3. High values of R^2 i.e., ≥ 0.8 are desired. The four function curves for data type denoted as Data 1, Data 2, Data 3, and Data 4 are produced using Eq. 12 through 15. For Data 3 and Data 4 function curves, their lower 95% confidence on fit curves; and their 90% lower data bound with 95% confidence i.e., lower 90/95% P/C curves are also shown. For forward case, target flaw size $x_{c2,90/95}^{target}$ is the input flaw size such that,

$$x_{c2,90/95}^{target} \leq x_{c2,90/95}^{req}. \tag{26}$$

It is indicated by a vertical line through diamond markers. Vertical line through triangle markers is the output flaw size, i.e. the predicted demonstration flaw size $x_{c1,90/95}^{demo}$ that needs to be detected with minimum 90/95% P/C. Theoretical P/C 90/95% induced flaw size $x_{c2,90/95}^{theo}$ in part is indicated by a triangle located on the Data 4 lower 90/95% P/C curve. This is a theoretical estimate. It is only possible in the simulation exercise where Data 4 curve with lower 90/95% P/C is known. Here, the following condition needs to be true with 95% confidence to indicate that the transfer function model is validated.

$$\Delta x_{c2}^{F} = x_{c2,90/95}^{target} - x_{c2,90/95}^{theo} \geq 0 \text{ with} > 95\% \text{ confidence.} \tag{27}$$

This condition can be assessed using repetitive sampling and Δx_{c2}^{F} is computed. Distribution of Δx_{c2}^{F} is analyzed to assess confidence and validate the transfer function model for the chosen case and data. If the signal response transfer relationships model is accepted and transfer function model is validated, then the difference between the input flaw size and the output flaw size needs to exceed a certain set limit to indicate that the flaw size detectability demonstration is necessary.

$$x_{c2,90/95}^{target} - x_{c1,90/95}^{demo} > \delta x_{lim,F}, \tag{28}$$

where, $\delta x_{lim,F}$ = minimum limit for requiring transfer function validation of NDE procedure. The above calculation does not require simulated data and it can be performed using actual Data 1 and Data 2 sample data. Forward model equations will be provided in later sections. The $\delta x_{lim,F}$ should be larger than the measurement error and should be a chosen value based on risk assessment by engineering especially by fracture control engineering. More on Eq. (28) will be discussed later.

In this example, condition of Eq. (27) is met approximately for a single sampling calculation. A dotted horizontal line indicates decision threshold that is calculated in the transfer function analysis. Calibration can be performed using appropriate size flaw of Data 1 or Data 2 type. These are indicated by * in Fig. 3. The calibration flaw response would provide nominal signal response that would be equal to the transfer function calculated decision threshold. Alternately, calibration flaw can be of Data 1 or Data 2 type and of target flaw size. The decision threshold would then be achieved by choosing correct percentage that is much less than 100% of the calibration flaw signal response.

5. METHOD FOR ASSESSING EFFECTIVITY OF INVERSE TRANSFER FUNCTION MODEL

Having accepted the signal response transfer relationships model, simulated data will be used to assess effectivity of the inverse transfer function model as an example.

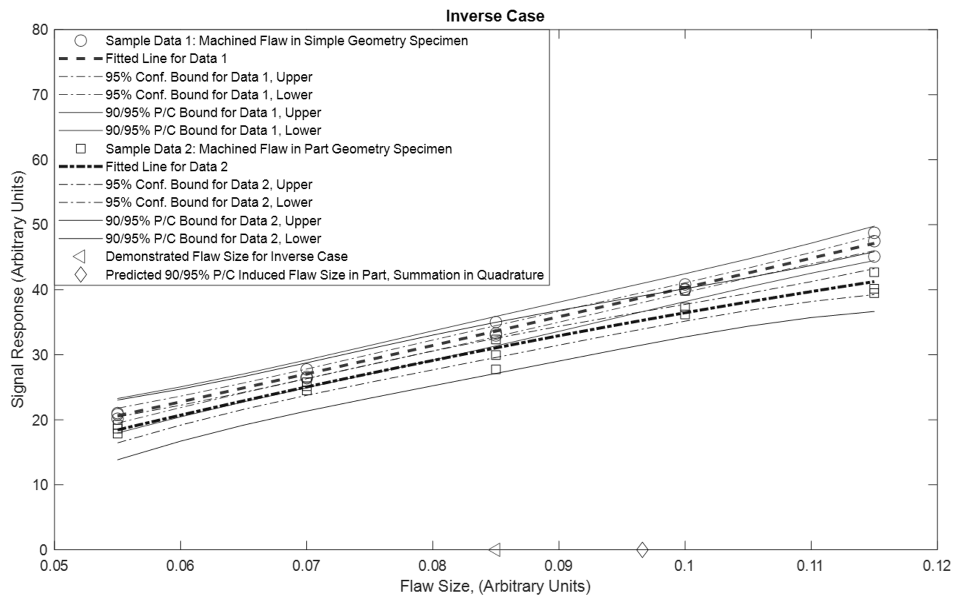

Fig. 4: Fitted second order polynomials through sample Data 1 and Data 2

Here, sampling protocol for Data 1 and Data 2 needs to be selected. The flaw sizes in the sample will be equally spaced. As an example, 5 flaw sizes are chosen and 3 replicates at each flaw size are chosen. For curve fitting through these data points, either a straight line or a second order polynomial is available. Second order polynomial is chosen in this example. Use of second order polynomial assumes that data does not have an inflection point. Therefore, the sample flaw size range should be chosen carefully. Fig. 4 and 5 illustrate the example of inverse case.

Regression coefficient R^2 values for Data 1 sample and Data 2 samples are provided in Fig 5. High values of R^2 i.e., ≥ 0.8 are desired. The four function curves for Data 1, Data 2, Data 3, and Data 4 are produced using Eq. (12) through Eq. (15). Error function is fitted through Data 3 and Data 4 function data. Data 3 and Data 4 fitted function curves, their 95% confidence on fit curves, and their 90% lower data bound with 95% confidence i.e., lower 90/95% P/C are also shown in Fig. 5. For inverse case, demonstration flaw size $x_{c1,90/95}^{demo}$ is the input flaw size. It is indicated by a vertical line through triangle markers. Vertical line through diamond markers is the output flaw size, i.e., the predicted or estimated flaw size $x_{c2,90/95}^{est}$ with 90/95% P/C.

Theoretical P/C 90/95% induced flaw size $x_{c2,90/95}^{theo}$ in part is indicated by triangle marker located on the Data 4 lower 90/95% P/C curve. This is considered to be a theoretical estimation, as it is only possible to estimate it in the simulation exercise where Data 4 curve with lower 90/95% P/C is known. Here, the following condition needs to be true with 95% confidence to indicate that the transfer function model is validated.

$$\Delta x_{c2}^{I} = x_{c2,90/95}^{est} - x_{c2,90/95}^{theo} \geq 0 \text{ with > 95\% confidence} \tag{29}$$

This condition can be assessed using repetitive sampling and Δx_{c2}^{I} is computed. Distribution of Δx_{c2}^{I} can be analyzed to assess confidence and validate the transfer function model. However, this exercise has limitations, as the $x_{c2,90/95}^{theo}$ is also dependent upon effectivity or variability of the curve fit function. Therefore, validation of transfer function model may mean acceptance of risk in the analysis to Eq. (29) criteria and qualitative assessment of how much the transfer function results may be deviating from the unknown 90/95 POD flaw size. Therefore, reliability to minimum 90/95% P/C is not proven directly in transfer function approach.

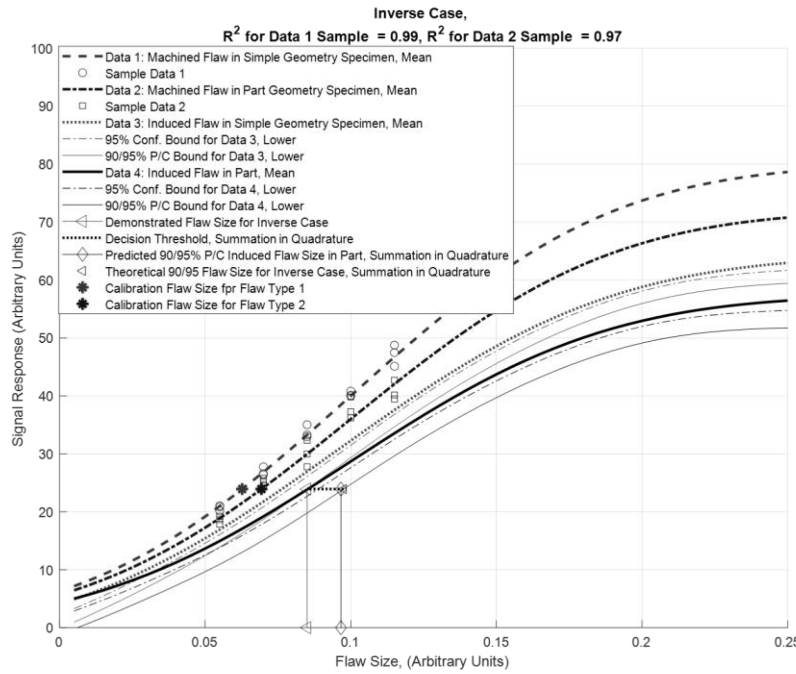

Fig. 5: Sample Data 1 and Data 2 overlaid on the respective mean curves and analysis for inverse case

If the signal response transfer relationships model is accepted and transfer function model is validated, then the difference between the input flaw size and the output flaw size needs to exceed a certain set limit to evaluate whether the inverse transfer function analysis was necessary.

$$x_{c2,90/95}^{est} - x_{c1,90/95}^{demo} > \delta x_{lim,I}, \tag{30}$$

where, $\delta x_{lim,I}$ = minimum limit for requiring transfer function validation of NDE procedure. In practice, the inverse case analysis is performed to meet following condition.

$$x_{c2,90/95}^{est} \leq x_{c2,90/95}^{req}. \tag{31}$$

In this example, condition of Eq. (30) is met approximately for a single sampling calculation. However, if there is an adequate margin to meet Eq. (31), then $x_{c2,90/95}^{req}$ may be acceptable "as is" for fracture control analysis. A dotted horizontal line indicates decision threshold that is calculated in the transfer function analysis. Calibration can be performed using appropriate size flaw of Data 1 or Data 2 type. These are indicated by * in Fig. 5. The calibration flaw response would provide nominal signal response that would be equal to the transfer function calculated decision threshold. Alternately, calibration flaw can be of type Data 1 or Data 2 and of target flaw size. The decision threshold would then be achieved by choosing correct percentage that is much less than 100% of the calibration flaw signal response.

6. FORWARD TRANSFER FUNCTION MODELS

Since samples of Data 1 and Data 2 are used in transfer function, Eq. (20) is interpreted as follows for both forward and inverse models,

$$\bar{y}_{c2}^{fit} = \frac{\bar{y}_{c1}^{fit}\bar{y}_{e2}^{fit}}{\bar{y}_{e1}^{fit}}. \tag{32}$$

Forward case calculation follows calculations in a sequence from point A to point F i.e., point A ---> point B ---> point C ---> point D ---> point E ---> point F in Fig. 6. From point A to point B, the transfer is described as flaw type (e.g., crack to EDM) transfer on signal response for same flaw size. From point B to point C, it is described as geometry (e.g., part to flat plate) transfer on flaw size for same signal response. From point D to point E, it is described as flaw type (e.g., EDM to crack) transfer on signal response at same flaw size. See Fig. 6. Uncertainty in flaw size at each point of calculation is used to calculate compound uncertainty in the resulting calculation.

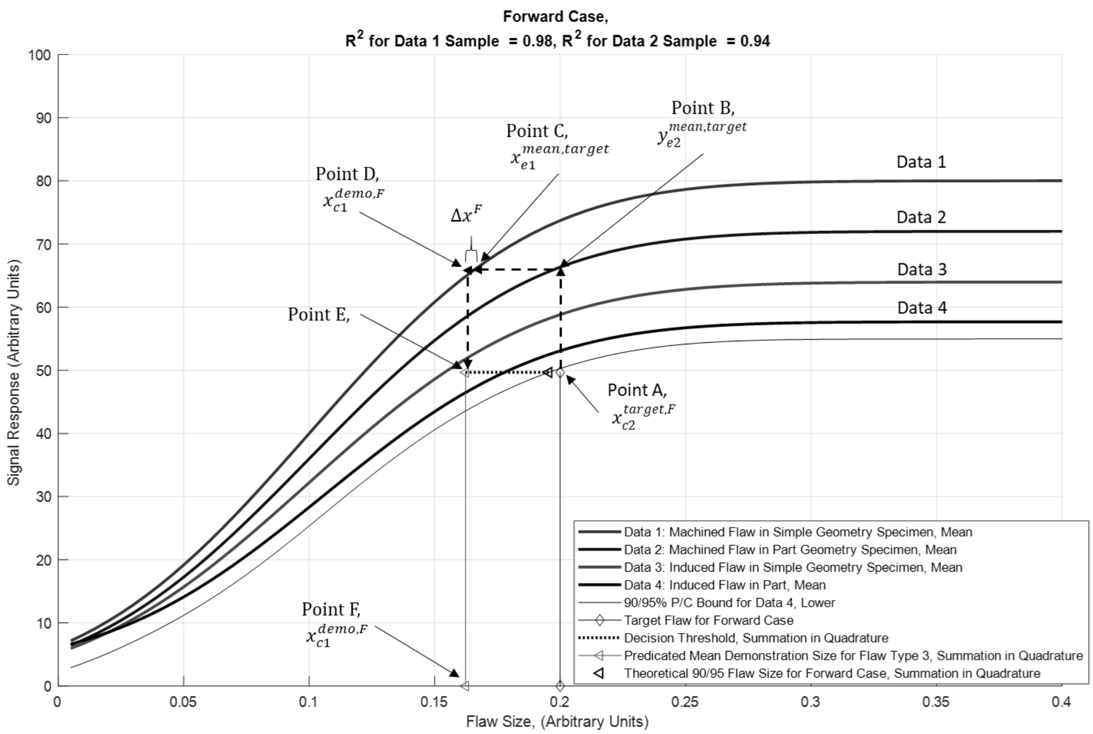

Fig. 6: Sequence of forward transfer function calculations

Using x-coordinate $x_{c2}^{target,F}$ of point A, point B y-coordinate or signal response of point B (on Data 2 curve) is calculated as follows,

$$y_{e2}^{mean,target} = interp\left(x, y_{e2,}^{fit} x_{c2}^{target,F}\right), \tag{33}$$

where *interp* = interpolation function. First two variables are linear arrays defining the fit curve while the third variable has a single value. Uncertainty in x-coordinate or flaw size, which is equivalent to uncertainty in y-coordinate at point B, is calculated as,

$$\Delta x_{e2}^{target,F} = interp\left(y_{e2}^{95C}, x, y_{e2}^{mean,target}\right) - x_{e2}^{mean,target}\ . \tag{34}$$

y_{e2}^{95C} is a curve for 95% lower confidence bound to Data 2 y_{e2}^{fit} curve. Next, x-coordinate or flaw size of point C (on Data 1 curve) is calculated as follows,

$$x_{e1}^{mean,target} = interp\left(y_{e1,}^{fit} x, y_{e2}^{mean,target}\right). \tag{35}$$

Uncertainty in x-coordinate or flaw size which is equivalent to uncertainty in y-coordinate at point C is calculated as,

$$\Delta x_{e1}^{target,F} = interp\left(y_{e1}^{95C}, x, y_{e2}^{mean,target}\right) - x_{e1}^{mean,target}. \tag{36}$$

There is uncertainty in locating point E on Data 3 curve. This uncertainty is calculated using following two equations.

$$y_{c1}^{mean,target} = interp\left(x, y_{c1,}^{fit} x_{e1}^{mean,target}\right), \text{ and} \tag{37}$$

$$\Delta x_{c1}^{target,F} = interp\left(y_{c1}^{95C}, x, y_{c1}^{mean,target}\right) - x_{e1}^{mean,target}. \tag{38}$$

Because of sequential calculation, uncertainty in x-coordinate of point B carries over and adds to uncertainty in x-coordinate of point C. Using central limits theorem, uncertainty at point C is given by,

$$\Delta x^F = \sqrt{\left(\Delta x_{e1}^{target,F}\right)^2 + \left(\Delta x_{e2}^{target,F}\right)^2 + \left(\Delta x_{c1}^{target,F}\right)^2}. \tag{39}$$

However, Data 3 $y_{c1,}^{fit}$ and y_{c1}^{95C} may not be known and $\Delta x_{c1}^{target,F}$ may be unknown. Also, in the initial evaluation, Data 3 may not be available at all and $y_{c1,}^{fit}$ and y_{c1}^{95C} cannot be estimated. In this case, an assumption as follows can be made,

$$\Delta x_{e2}^{target,F} \leq \Delta x_{c1}^{target,F}. \tag{40}$$

Using above condition, Eq. (39) simplifies to,

$$\Delta x^F \geq \sqrt{\left(\Delta x_{e1}^{target,F}\right)^2 + 2\left(\Delta x_{e2}^{target,F}\right)^2} \text{ for } \Delta x_{e2}^{target,F} \leq \Delta x_{c1}^{target,F}. \tag{41}$$

Demonstration flaw size $x_{c1}^{demo,F}$ is calculated as follows,

$$x_{c1}^{demo,F} = x_{e1}^{mean,target} - \Delta x^F. \tag{42}$$

Depending upon whether an approximate or calculated value of Δx^F is used, the results and confidence in the results are affected. Value of Eq. (28) should be greater than the uncertainty in the estimation of $x_{c1}^{demo,F}$. This is given by following condition,

$$\delta x_{lim,F} > \Delta x^F. \tag{43}$$

It should be remembered that the transfer function model may not work close to the saturation limits i.e., lower and upper limits due to non-linearity in signal response. Therefore, it is important to run the simulation exercise to understand whether application of transfer function model and sampling regime is likely to be successful. The paper provides method to determine whether transfer function validation is necessary. If transfer function validation is deemed necessary, then designing specimens for Data 1 and Data 2 samples and Data 3 demonstration set is needed. Method for designing sampling of Data 1 and Data 2 for transfer function method is provided. Using signal response data from Data 1 and Data 2 samples and above equations, the forward transfer function analysis can be performed. Generally, the model should work well if data can be modeled with linear fits. Linear fit is not possible near saturation limits where it would be advisable to check effectivity of the model using simulation.

7. INVERSE TRANSFER FUNCTION MODELS

Inverse case calculation follows calculations in a sequence from point A to point F i.e. point A ---> point B ---> point C ---> point D ---> point E ---> point F in Fig. 7. From point A to point B, the transfer is described as flaw type (e.g. crack to EDM signal response) transfer. From point B to point C the transfer is described as geometry (e.g. part to flat plate flaw size) transfer. From point D to point E the transfer is described as flaw type (e.g. EDM to crack signal response) transfer. See Fig. 7.

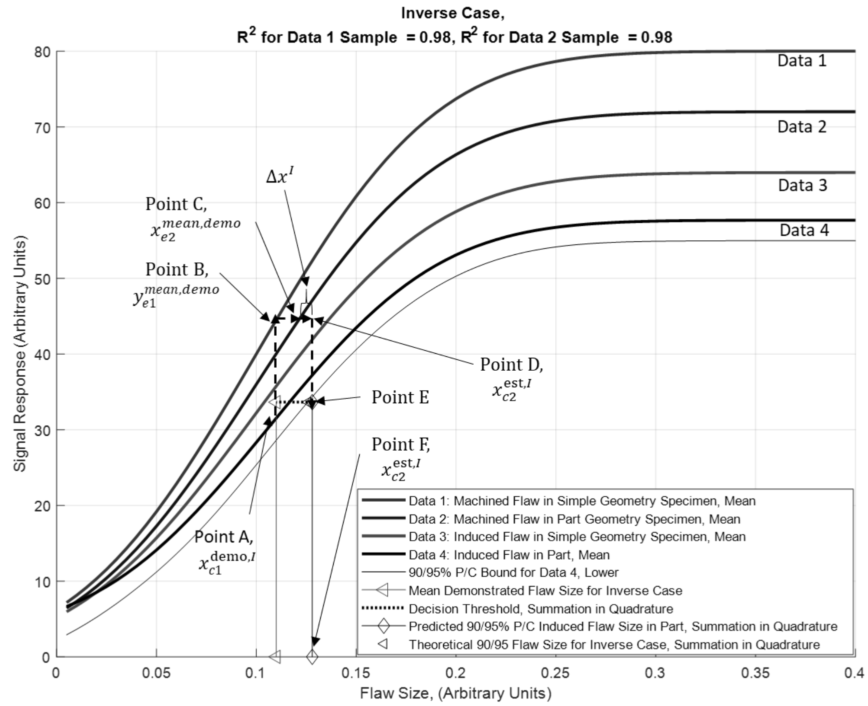

Fig. 7: Sequence of inverse transfer function calculations

Using x-coordinate of point A $x_{c1}^{demo,I}$, point B y-coordinate or signal response (on Data 1 curve) is calculated as follows,

$$y_{e1}^{mean,demo} = interp\left(x, y_{e1,}^{fit} x_{c1}^{demo,I}\right). \tag{44}$$

Uncertainty in x-coordinate or flaw size, which is equivalent to uncertainty in y-coordinate at point B, is calculated as,

$$\Delta x_{e1}^{demo,I} = interp\left(y_{e1}^{95C}, x, y_{e1}^{mean,demo}\right) - x_{c1}^{demo,I}\ . \tag{45}$$

y_{e1}^{95C} is a curve for 95% lower confidence bound to Data 1 curve y_{e1}^{fit}. Next x-coordinate or flaw size of point C (on Data 2 curve) is calculated as follows,

$$x_{e2}^{mean,demo} = interp\left(y_{e2,}^{fit} x, y_{e1}^{mean,demo}\right). \tag{46}$$

Uncertainty in x-coordinate or flaw size which is equivalent to uncertainty in y-coordinate at point C is calculated as,

$$\Delta x_{e2}^{demo,I} = interp\left(y_{e2}^{95C}, x, y_{e1}^{mean,demo}\right) - x_{e2}^{mean,demo}. \tag{47}$$

There is uncertainty $\Delta x_{c1}^{demo,I}$ in locating the point A i.e. $x_{c1}^{demo,I}$ on the Data 3 curve. It can be calculated using following two equations.

$$y_{c1}^{mean,demo} = interp\left(x, y_{c1,}^{fit} x_{e1}^{demo,I}\right), \text{ and} \tag{48}$$

$$\Delta x_{c1}^{demo,I} = interp\left(y_{c1}^{95C}, x, y_{c1}^{mean,demo}\right) - y_{c1}^{mean,demo}. \tag{49}$$

Because of sequential calculation, uncertainty in x-coordinate of point A carries over to and adds to uncertainty in x-coordinate of point B. Uncertainty in x-coordinate of point B carries over and adds to uncertainty x-coordinate of point C. Uncertainties in locating points A, B and C have effect on uncertainty in locating point E and this effect should be modeled using summation of quadrature of individual uncertainties using central limits theorem. Uncertainty at point E is given by,

$$\Delta x^{I} = \sqrt{\left(\Delta x_{e1}^{demo,I}\right)^2 + \left(\Delta x_{e2}^{demo,I}\right)^2 + \left(\Delta x_{c1}^{demo,I}\right)^2}\ . \tag{50}$$

However, $y_{c1,}^{fit}$ and y_{c1}^{95C} may not be known and $\Delta x_{c1}^{demo,I}$ may be unknown. The uncertainty $\Delta x_{c1}^{demo,I}$ is included in $x_{c1}^{demo,I}$ but value may not be known but it is recommended to add this uncertainty in the summation of quadrature of uncertainties. See Eq. (50). Incorporating $\Delta x_{c1}^{demo,I}$ in Eq. (50) is more conservative. Data 3 may not be available at all and $y_{c1,}^{fit}$ and y_{c1}^{95C} cannot be estimated. In this case, an assumption as follows can be made,

$$\Delta x_{e2}^{demo,I} \leq \Delta x_{c1}^{demo,I}. \tag{51}$$

With above assumption, Eq. (50) is rewritten as,

$$\Delta x^{I} \ \geq \sqrt{\left(\Delta x_{e1}^{demo,I}\right)^2 + 2\left(\Delta x_{e2}^{demo,I}\right)^2} \text{ for } \Delta x_{e2}^{demo,I} \leq \Delta x_{c1}^{demo,I}. \tag{52}$$

Estimated reliably detectable flaw size $x_{c2}^{est,I}$ is calculated as follows,

$$x_{c2,90/95}^{est} = x_{e2}^{mean,demo} + \Delta x^{I} \ . \tag{53}$$

Depending upon whether an approximate or calculated value of Δx^{I} is used, the results and confidence in results are affected. Value of Eq. (30) should be greater than the uncertainty in the estimation of $x_{c1}^{demo,F}$. This is given by following condition,

$$\delta x_{lim,I} > \ \Delta x^{I} \ . \tag{54}$$

Generally, the model should work well if data can be modeled with linear fit. Linear fit is not possible near saturation limits where it would be advisable to check effectivity of the model using simulation.

8. EXAMPLE OF TRANSFER FUNCTION CALCULATIONS

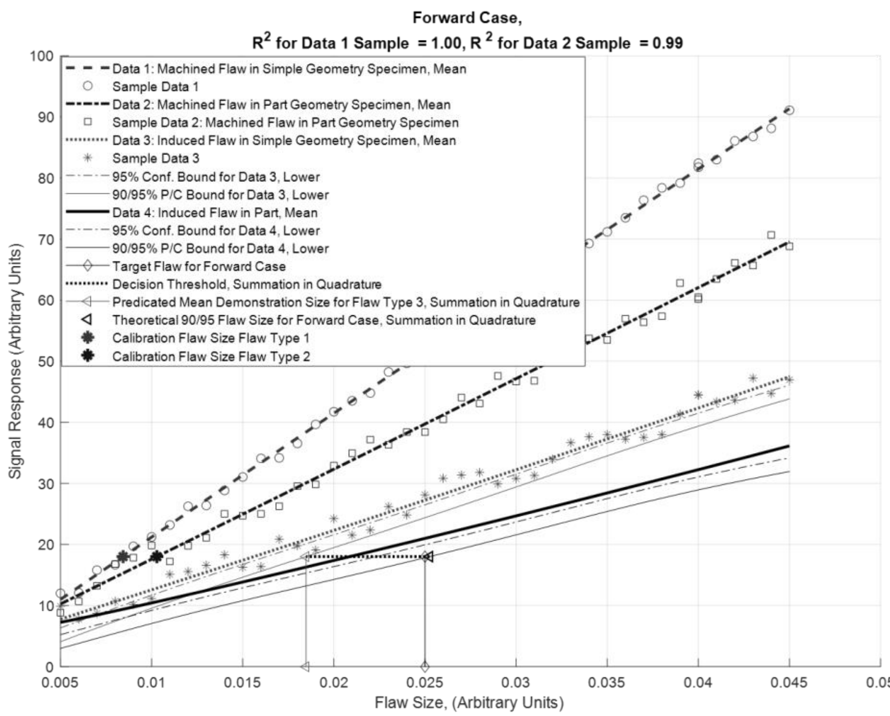

Fig. 8: Example of forward case using simulated data

Examples of forward and inverse case transfer function analysis is provided below. Here, simulated data is used as an input. Resulting flaw sizes for both forward and inverse case are calculated using Data 1 and Data 2 only. Eq. (41) is used for forward case and Eq. (52) is used for inverse case. However, Data 3 is shown in Fig. 8 and Fig. 10 for showing effectivity of the calculations. Both calculations seem to show approximately good results to Eq. (27) for forward case and to Eq. (29) for inverse case. Note that data is identical in Fig. 8 through Fig. 11.

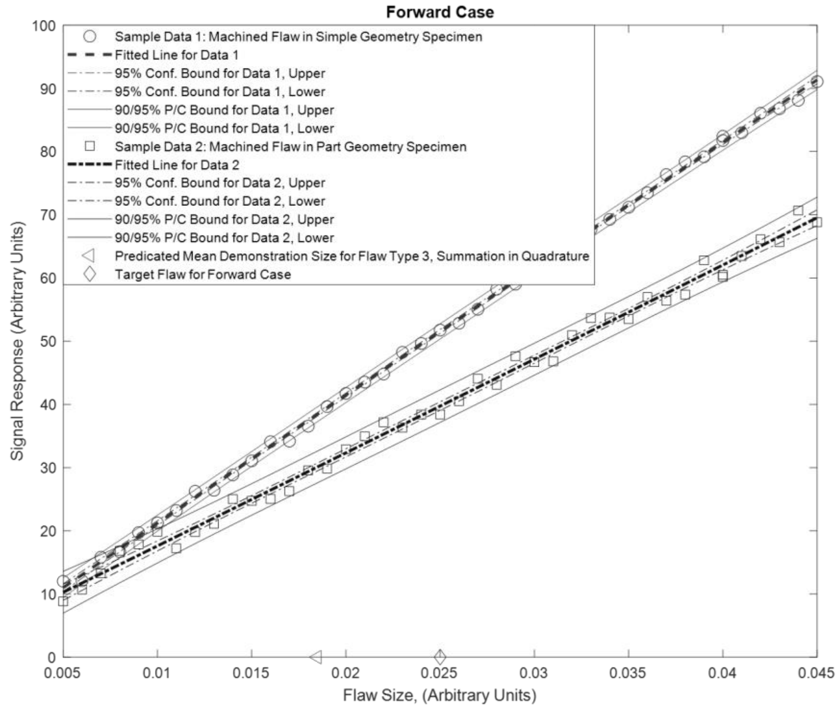

Fig. 9: Example of forward case using simulated data of Data 1 and Data 2 only

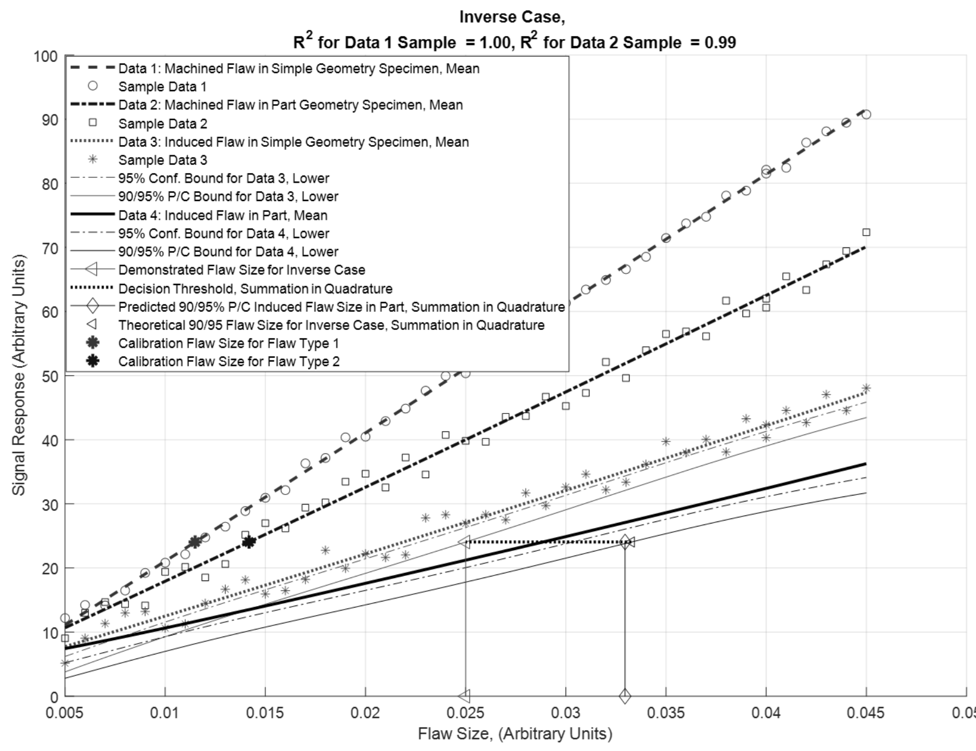

Fig. 10: Example of inverse case using simulated data

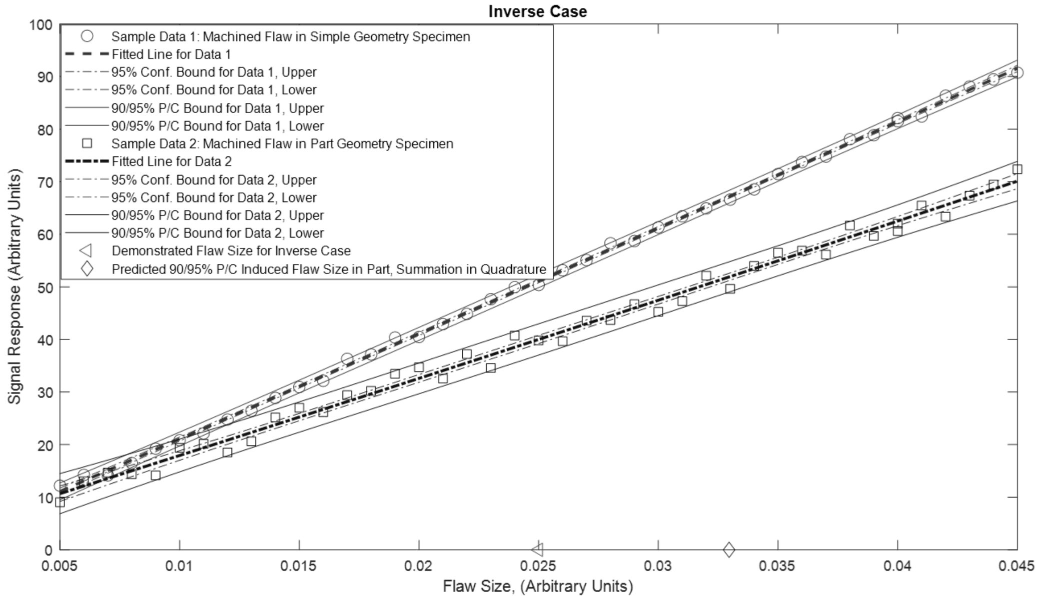

Fig. 11: Example of inverse case using Data 1 and Data 2 only

9. CONCLUSIONS

The signal response transfer relationships model is devised first and then transfer function models have been devised for linear response signals with flaw size. Assuming the signal response transfer relationships model is applicable to the NDE application, transfer function forward or inverse methods have been devised with an objective to provide adequate confidence to the assumed signal response transfer relationships model. If non-linearity is seen in the sampled data, a transfer function simulation method can be used to assess applicability and confidence in the transfer function method. Transfer function method may provide acceptable results for signal response data that can be modeled with linear fit. For non-linear data, transfer function simulation is advised to assess applicability of transfer function method. The transfer function method may be assessed using simulation to check whether the resulting target size or demonstration size provide adequate confidence to the assumed signal response transfer relationships model. Because of lack of signal response data from induced flaws in real part, 90/95% POD/confidence cannot be demonstrated directly. Therefore, the transfer function approach is a risk assessment approach. Both, the signal response transfer relationships model and the transfer function model, are important in managing risk in results provided by transfer function method of NDE technique qualification or assessment. The signal response transfer relationships model needs to be validated with empirical data and then transfer function model needs to be validated for desired POD and confidence on case-by-case basis.

REFERENCES

[1] MIL-HDBK-1823A, “Nondestructive Evaluation System Reliability Assessment,” Department of Defense, USA, (2009).

[2] Annis, Charles, “mh1823 POD Software V5.2.1,” Statistical Engineering, http://www.statisticalengineering.com/mh1823/, (2016).

[3] ASTM E 2862-12, “Standard Practice for Probability of Detection for Hit/Miss Data,” ASTM International, (2012).

[4] Rummel Ward D., “Recommended Practice for Demonstration of Nondestructive Evaluation (NDE) Reliability on Aircraft Production Parts,” Materials Evaluation, August Issue 40 pp 922, (1988).

[5] NIST/ Dataplot, “SD Confidence Limits,” https://www.itl.nist.gov/div898/software/dataplot/refman1/auxillar/sdconfli.htm

[6] NIST/SEMATECH e-Handbook of Statistical Methods, Section 7.2.6.3, May 29, 2020, https://doi.org/10.18434/M32189, https://www.itl.nist.gov/div898/handbook/prc/section2/prc263.htm

[7] Koshti, A. M., “Using requirements on merit ratios for assessing reliability of NDE flaw detection,” SPIE Smart Structures and NDE, Proc. SPIE 11593, (2021).
[8] Koshti, A. M., “Using requirements on merit ratios for assessing reliability of NDE flaw detection in multi-hit detection in digital radiography,” SPIE Smart Structures and NDE, Proc. SPIE 11593, (2021).
[9] Koshti, A. M., "Assessing risk due to small sample size in probability of detection analysis using tolerance intervals," SPIE Smart Structures and NDE, Proc. SPIE 12048, Health Monitoring of Structural and Biological Systems XVI, 1204817 (2022).
[10] Koshti, A. M., “Assessment of flaw detectability using transfer function,” SPIE Smart Structures and NDE, Proc. SPIE 11592, (2021).
[11] Koshti, A. M., “Modeling reliability of an NDE method providing a C-scan, a case of flaw field simulation,” SPIE Smart Structures and NDE, Proc. SPIE 11593, (2021).
[12] Koshti, A. M., “Optimizing raster scanning parameters in nondestructive evaluation using simulation of probe sensitivity field,” SPIE Smart Structures and NDE, Proc. SPIE 11592, (2021).
[13] Koshti, A. M., “Assessing Visual and System Flaw Detectability in Nondestructive Evaluation,” SPIE Smart Structures and NDE, SPIE 11592, (2021).
[14] Koshti, A. M., “Probability of Detection Analysis in Multi-Hit Flaw Detection,” SPIE Smart Structures and NDE, SPIE 11594, (2021).
[15] Koshti Ajay, Parker Peter, Forsyth David, Suits, Michael, Walker James, and Prosser, William, “Guidebook for Limited Sample Probability of Detection (LS-POD) Demonstration for Single Hit Nondestructive Evaluation (NDE) Methods,” NASA Langley Research Center, NESC-TI-20-01545, (2021).
[16] Koshti Ajay, Parker Peter, Forsyth David, Suits, Michael, Walker James, and Prosser, William, “Guidebook for Assessing Similarity and Implementing Empirical Transfer Functions for Probability of Detection (POD) Demonstrations for Single-Hit Nondestructive Evaluation (NDE) Methods”, NASA Langley Research Center, (2022).